Corrosion Behavior of Ceramics-Coated Hastelloy-XR Alloy in an Ar-SO2 Atmosphere

Materials Transactions, Vol. 44, No. 5 (2003) pp. 962 to 967

Corrosion Behavior of Ceramics-Coated Hastelloy-XR Alloy in an Ar–SO_2 Atmosphere

Rong Tu and Takashi Goto

Institute for Materials Research, Tohoku University, Sendai 980-8577, Japan

Glass lining and CVD (chemical vapor deposition) YSZ (yttria stabilized zirconia) coating were applied to improve the corrosion resistance of Hastelloy-XR alloy in an Ar–SO_2 atmosphere ($P_{SO_2} = 10$ kPa). A glass lining with the composition of 48 SiO_2–8 B_2O_3–6 Al_2O_3–11 CaO–25 BaO–2 ZnO (mass%) which protected the alloy substrate showed almost no crystallization and mass change below 1073 K, but suffered degradation at temperatures over 1173 K. The YSZ (8 mol% Y_2O_3) coating had a well-grown columnar structure and showed excellent corrosion resistance at 1273 K.

(Received November 27, 2002; Accepted March 19, 2003)

Keywords: *glass lining, ceramics coating, sulfur dioxide atmosphere, yttria stabilized zirconia, metal-organic chemical vapor deposition, Hastelloy-XR alloy*

1. Introduction

Since CO_2 emission due to the consumption of fossil fuels such as oil and coal is causing serious environmental problems, there are high expectations of hydrogen as a clean energy source. Although hydrogen can be produced by decomposing water, the decomposition temperature of pure water is very high, more than 3000 K. To date, hundreds of thermochemical processes such as the addition of acids and halogen,[1] to allow the decomposition of water at lower temperatures have been investigated, and successful continuous production of hydrogen gas in a closed cycle without emission of toxic chemicals has been recently achieved by the Iodine–Sulfur (IS) process.[2,3]

The IS process mainly consists of the decomposition reaction of H_2SO_4 around 1100 K, the Bunsen reaction around 400 K and the decomposition reaction of HI around 600 K.[4] SO_2 gas formed by the decomposition of H_2SO_4 would have the most corrosive effect on the structural materials of vessels and pipes. Although the bench scale setup for the IS process has been constructed with quartz glass and polymer materials;[5] commercially available ductile metallic materials should be employed to develop a large-scale chemical plant. Although no such metals can maintain their integrity in the SO_2 atmosphere,[5–7] Hastelloy-XR alloy appears to be a good candidate material because of its high mechanical strength and moderate corrosion resistance.[8] However, the corrosion resistance is insufficient for use in a harsh environment.[9]

In the present study, ceramics coatings such as silica system glass lining and YSZ (yttria stabilized zirconia) were applied to improve the corrosion resistance of Hastelloy-XR alloy, and the corrosion behavior of the ceramics-coated Hastelloy-XR alloy were investigated in an Ar–SO_2 atmosphere.

2. Experimental Method

Hastelloy-XR alloy (49 Ni–22 Cr–18 Fe–9 Mo–0.9 Mn–0.3 Si, mass%) with disk-shaped plates (10 mm in diameter by 1 mm in thickness) were used for specimens. The specimens were polished with an alumina paste (1 μm), and a thin oxide layer (about 1 μm in thickness) was formed by oxidation at 1230 K in an Ar–O_2 atmosphere (oxygen partial pressure (P_{O_2}) of 0.01 kPa) for 43 ks to obtain adhesive coating.[10] Various compositions of SiO_2–B_2O_3–Al_2O_3–MO (M: Ca, Ba, Zn) system glasses were used for the glass lining. The compositions examined in the present study are shown in Table 1. After weighing and mixing the source oxide powders, the mixed powders were melted, solidified and crushed into glass powders. Glass pastes were prepared by mixing the glass powders and an organic solvent (α-terpineol/ethyl cellulose = 10/1 in mass ratio). Hastelloy-XR alloy specimens were painted with the glass pastes and heat-treated at 400 K to evaporate the organic solvent. The specimens were then fired at 1200 to 1400 K in air for 1.8 ks to melt the glass.

Table 1 Composition of glasses (mass%).

Glass	SiO_2	B_2O_3	Al_2O_3	CaO	BaO	SrO	ZnO
A	91	3	2	2	2	—	—
B	81	12	5	—	2	—	—
C	70	5	2	9	14	—	—
D	65	9	5	14	—	—	7
E	53	5	13	12	11	6	—
F	50	15	10	—	25	—	—
G	48	8	6	11	25	—	2
H	34	24	4	12	12	—	14
I	23	22	6	3	19	—	27
J	11	44	6	2	3	—	34

CVD (chemical vapor deposition) was applied to prepare YSZ coating using $Zr(dpm)_4$ and $Y(dpm)_3$ (dpm: dipivaloylmethanate) as source materials. YSZ films were deposited on Hastelloy-XR alloy specimens at 1073 K and a total pressure (P_{tot}) of 0.8 kPa in a vertical-type CVD apparatus. Details of the experimental conditions have been reported elsewhere.[11]

Mass changes of the ceramics-coated alloys were measured by thermogravimetry at 1073 to 1273 K in an Ar–SO_2 atmosphere ($P_{SO_2} = 10$ kPa) for 43 ks. The surfaces and cross sections of the specimens after corrosion were examined by

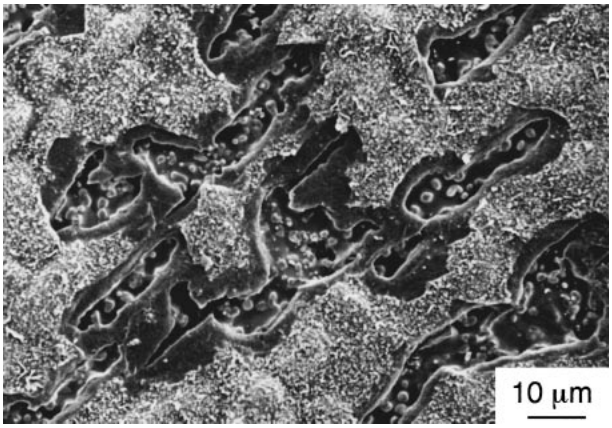

Fig. 1 Surface morphology of the scale formed on Hastelloy-XR after corrosion at 1073 K and $P_{SO_2} = 10$ kPa for 43 ks.

X-ray diffraction (XRD), scanning electron microscopy (SEM) and electron probe microanalysis (EPMA).

3. Results and Discussion

3.1 Corrosion behavior of Hastelloy-XR alloy

Figure 1 shows the surface morphology of the scale formed at 1073 K and $P_{SO_2} = 10$ kPa in an Ar–SO_2 atmosphere for 43 ks. The scale was about 1 μm in thickness and consisted of an inner Cr_2O_3 layer and an outer $Mn_{1.5}Cr_{1.5}O_4$ layer. The outer $Mn_{1.5}Cr_{1.5}O_4$ layer partially peeled, and then the inner Cr_2O_3 layer was observed as shown in Fig. 1. Not being protective in the corrosive atmosphere, the scales peeled off easily. Figure 2 depicts the surface and cross section of the scale formed at 1273 K and $P_{SO_2} = 10$ kPa for 43 ks. Many nodules were observed on the surface. The scale consisted of Fe_3O_4, $FeCr_2O_4$ and Cr_2O_3 layers from the surface to the substrate. Ni_3S_2 and CrS particles were observed in the Cr_2O_3 layer and in the grain boundary of the alloy substrate, respectively. The nodules were formed by partial exfoliation of the scale due to the difference of the thermal expansion among the Fe_3O_4, $FeCr_2O_4$ and Cr_2O_3 layers. A Ni–Fe–Mo phase scarcely containing Cr was detected in the substrate, and many pores were observed at the substrate/scale interface. These findings suggest that Cr diffused outward to form the scale.

3.2 Corrosion behavior of glass-lined Hastelloy-XR alloy

The thermal expansion coefficient (α) of borosilicate glasses (generally 50–90 $\times 10^{-7}$ K^{-1}) is less than that of Hastelloy-XR alloy (160×10^{-7} K^{-1}). Therefore, the α of glasses for lining should be increased as much as possible. It is known that the α of glasses increases with the addition of alkaline-earth metal elements, and thus the corrosion resistance would be improved by the addition of Al_2O_3 and/or ZnO.[12] In the present study, the use of SiO_2–B_2O_3–Al_2O_3–ZnO–MO (M: alkaline-earth metal) system glasses for glass lining was investigated.

Figure 3 represents the relationship between the composition and the corrosion trend for the glass lining. In an SiO_2 rich area (I), the melting points (or softening point) of glasses were too high (glass A and B) or the thermal expansion coefficients of glasses were too small (glass C and D) to obtain well-adhered glass lining. Figure 4 shows the appearance of glass B lining where the whole glass lining peeled off

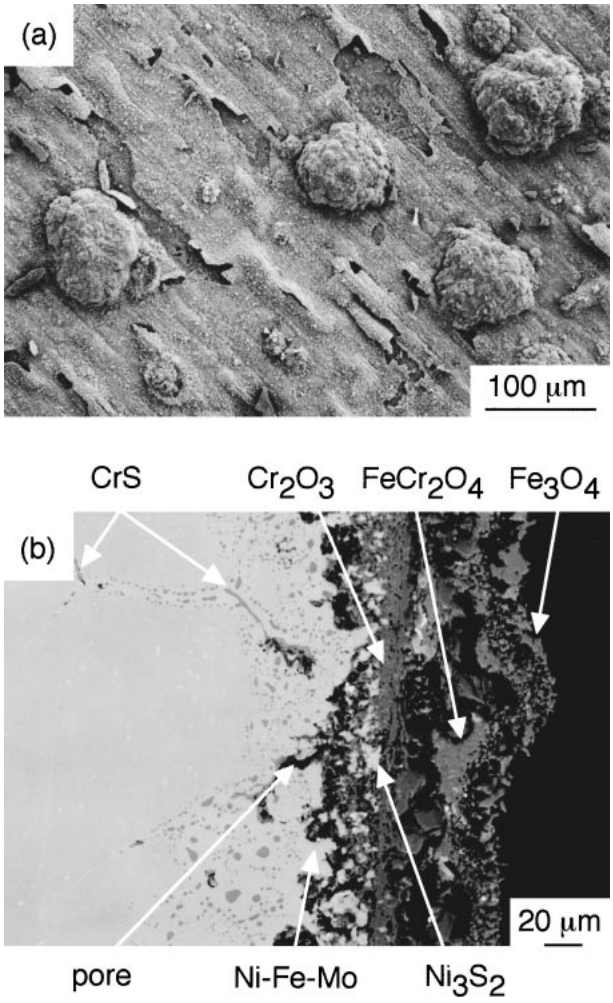

Fig. 2 Surface (a) and cross section (b) of the scale formed on Hastelloy-XR after corrosion at 1273 K and $P_{SO_2} = 10$ kPa for 43 ks.

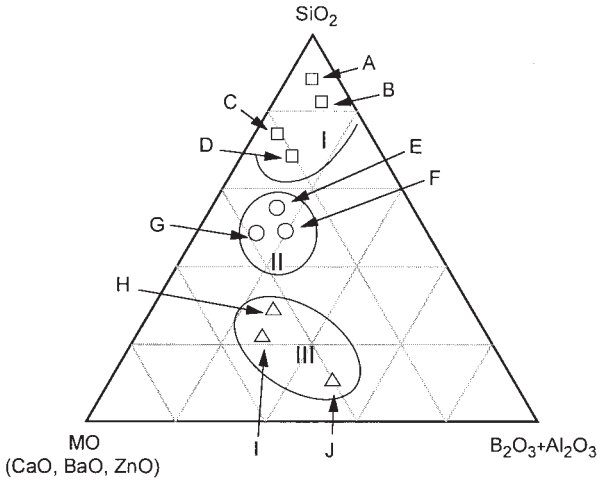

Fig. 3 Effect of composition on the corrosion trend of glass lining. (□: Cracked or peeled, ○: Good corrosion resistance, △: Bad corrosion resistance).

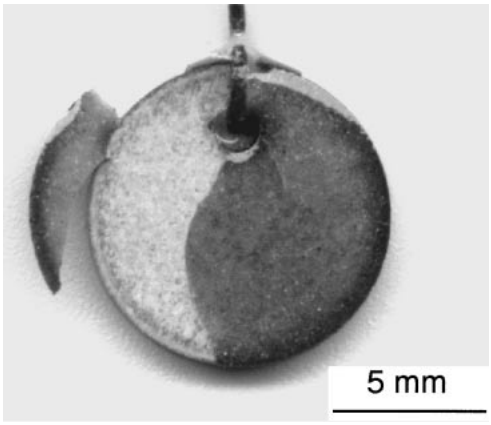

Fig. 4 Appearance of glass B lining Hastelloy-XR after cooling to room temperature.

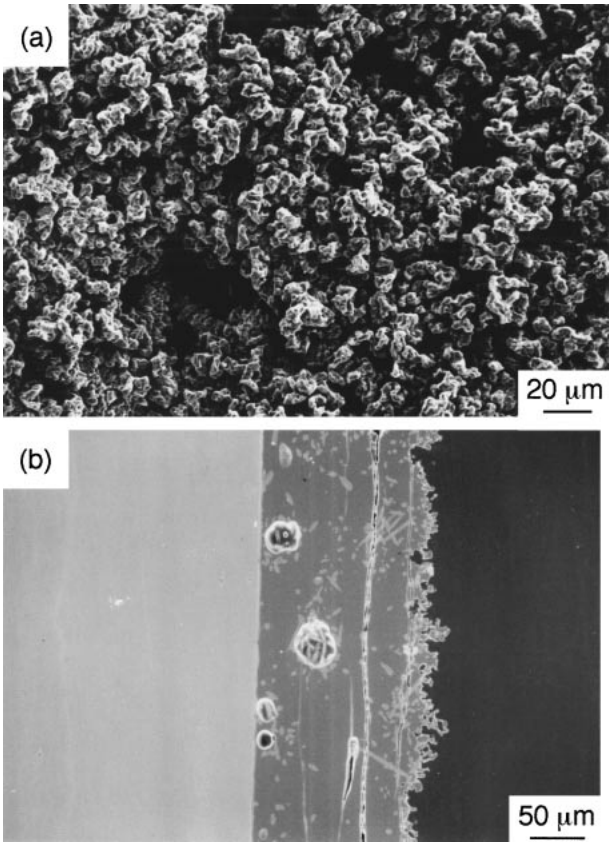

Fig. 5 Surface (a) and cross section (b) of glass I lining Hastelloy-XR after corrosion at 973 K and $P_{SO_2} = 10$ kPa for 43 ks.

from the alloy substrate. The glasses with the composition labeled as II and III in Fig. 3 were well-vitrified and adhered well to the alloy substrates. However, the corrosion resistance of the glasses labeled as III was too low. Figure 5 depicts the surface and cross section of glass I lining after corrosion at 973 K and $P_{SO_2} = 10$ kPa for 43 ks. The surface of the glass coating was significantly corroded, and partial crystallization and large cracks were observed in the glass lining.

The glass linings labeled as II in Fig. 3 showed good corrosion resistance and adhesion to the alloy substrate.

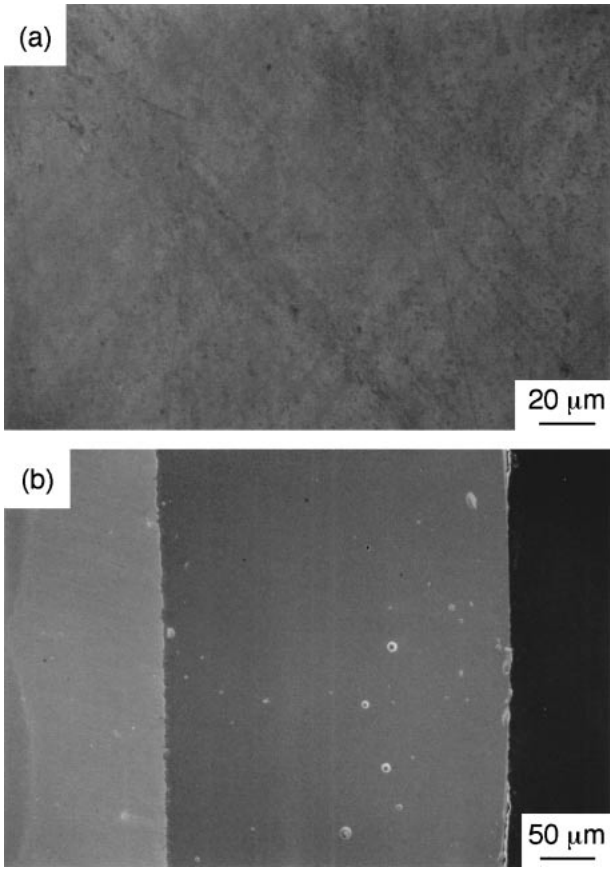

Fig. 6 Surface (a) and cross section (b) of glass G lining Hastelloy-XR after corrosion at 1073 K and $P_{SO_2} = 10$ kPa for 43 ks.

Figure 6 depicts the surface and cross section of glass G lining after corrosion at 1073 K and $P_{SO_2} = 10$ kPa for 43 ks. No degradation of the glass lining was observed, and no cracks and no crystallization were detected. Figure 7 represents the surface and cross section of glass G lining after corrosion at 1173 K and $P_{SO_2} = 10$ kPa for 43 ks. The surface of the glass lining about 1 μm in thickness was partially peeled off during cooling to room temperature. Figure 8 depicts the surface and cross section of glass G lining after corrosion at 1273 K and $P_{SO_2} = 10$ kPa for 43 ks. The surface of the glass lining became porous due to severe corrosion, and partial crystallization was observed in the glass.

Figure 9 shows the X-ray diffraction patterns of the surface of glass G lining after corrosion at 1073 K, 1173 K and 1273 K at $P_{SO_2} = 10$ kPa for 43 ks. A broad peak was observed at 1073 K, indicating no crystallization of the glass lining. Sharp peaks identified as $BaSO_4$ were observed after corrosion at 1273 K. The equilibrium solid products of glass G by corrosion in Ar–SO_2 were calculated by the computer code SOLGASMIX-PV.[13] Figure 10 demonstrates the mass fraction of solid products as a function of P_{SO_2} at 1273 K. Glass G lining would be corroded forming mainly $BaSO_4$ and $CaSO_4$ over $P_{SO_2} = 100$ Pa. As shown in Fig. 9, however, $CaSO_4$ was not identified in the experiments. The formation of $CaSO_4$ might be hindered due to some kinetic factor. It is concluded that the glass G lining has corrosion resistance in an SO_2 atmosphere below 1073 K; however, the corrosion resistance is not sufficient over 1173 K.

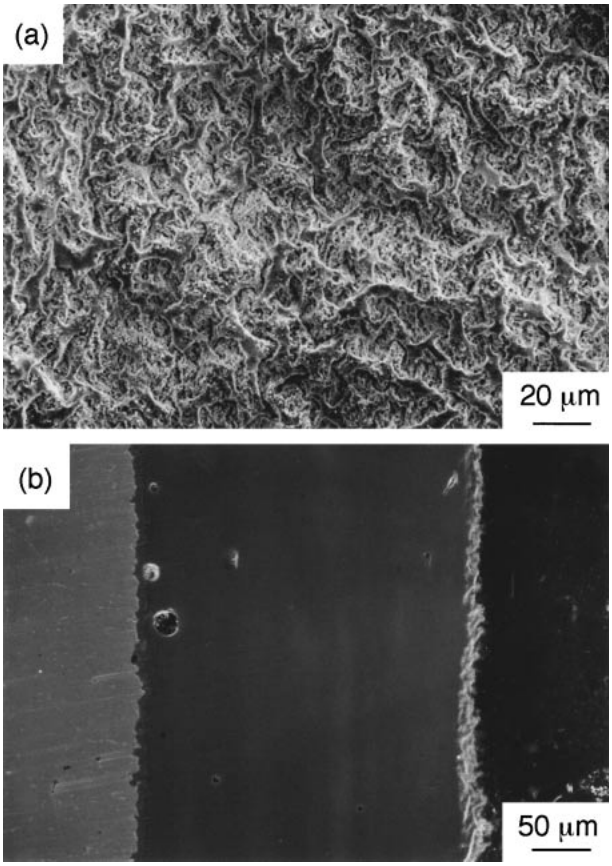

Fig. 7 Surface (a) and cross section (b) of glass G-coated Hastelloy-XR after corrosion at 1173 K and $P_{SO_2} = 10$ kPa for 43 ks.

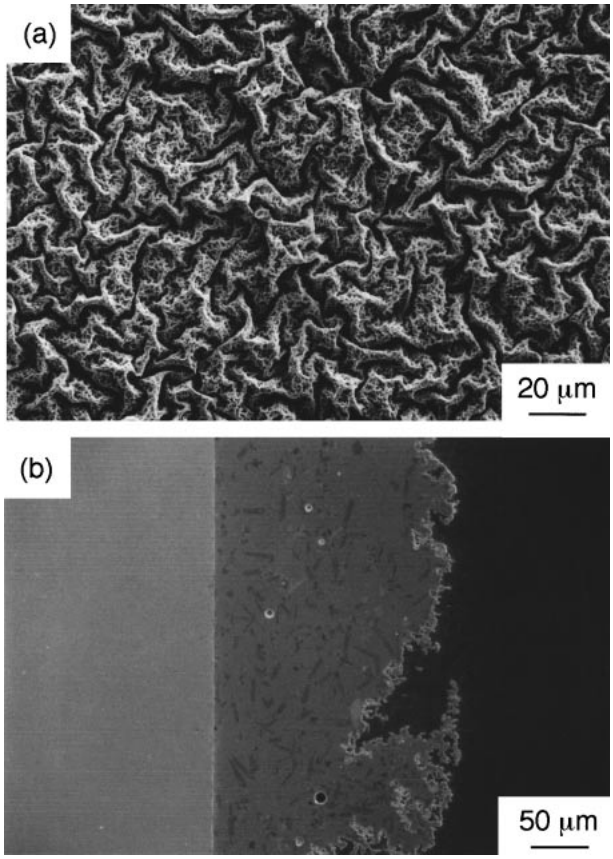

Fig. 8 Surface (a) and cross section (b) of glass G-coated Hastelloy-XR after corrosion at 1273 K and $P_{SO_2} = 10$ kPa for 43 ks.

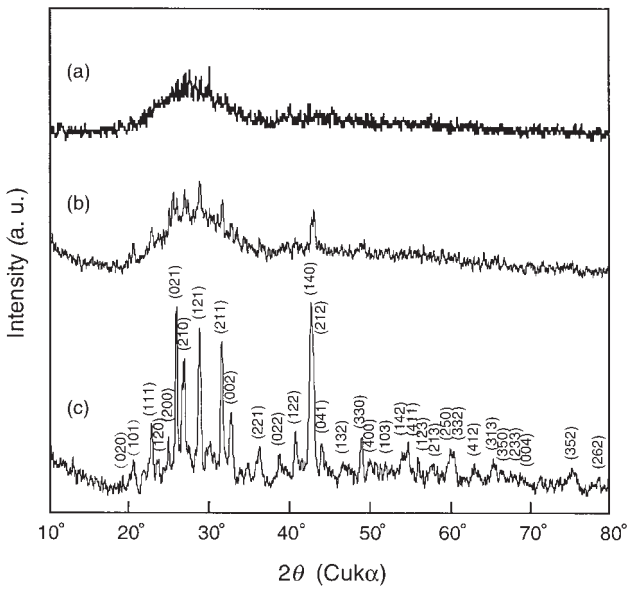

Fig. 9 X-ray diffraction patterns of glass G lining after corrosion at (a) 1073, (b) 1173 and (c) 1273 K at $P_{SO_2} = 10$ kPa for 43 ks. (Indexes are for $BaSO_4$).

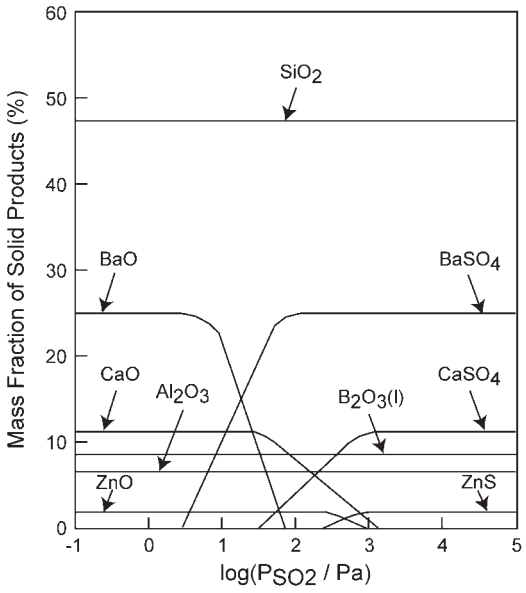

Fig. 10 Calculated mass fraction of solid products for glass G after corrosion as a function of P_{SO_2} at 1273 K.

3.3 Corrosion behavior of YSZ-coated Hastelloy-XR alloy

YSZ films were prepared on quartz glass substrates to examine the texture of coatings. Figures 11(a) and (b) demonstrate the cross sections of the fractured surface and the polished surface of YSZ films prepared on quartz glass and alloy substrates, respectively. The YSZ films had a columnar structure and adhered well to the substrates. The deposition conditions of the YSZ films are summarized in Table 2. The Y_2O_3 content of the YSZ film was determined as 8 mol% by EPMA analysis. Figure 12 shows the X-ray

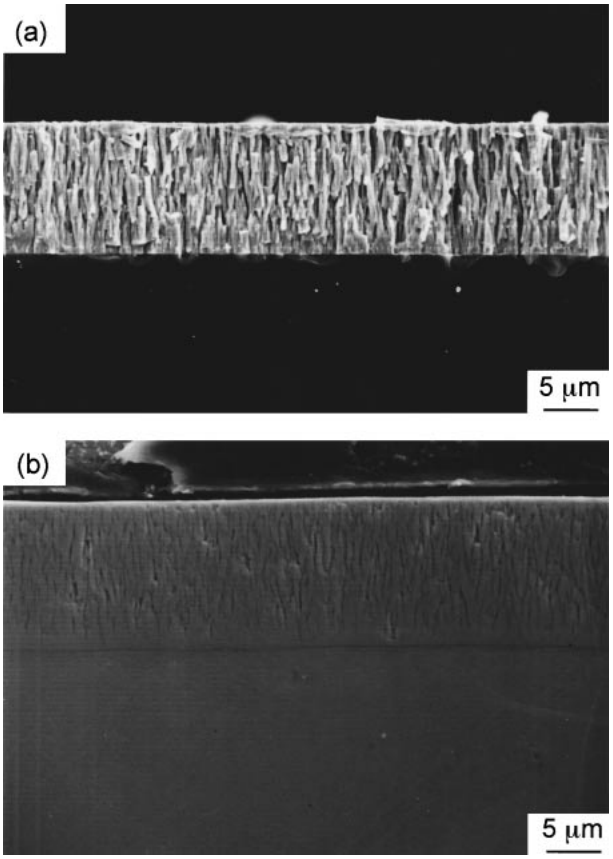

Fig. 11 Cross sections of YSZ films deposited on fused quartz (a) and Hastelloy-XR alloy (b). ($T_{Zr} = 593$ K, $T_Y = 433$ K, $P_{tot} = 0.8$ kPa, $T_{dep} = 1073$ K, $t_{dep} = 0.9$ ks).

Table 2 Deposition conditions for YSZ films.

Evaporation temperature of precursors	
$Zr(dpm)_4$ (T_{Zr})	593 K
$Y(dpm)_3$ (T_Y)	433 K
Deposition temperature (T_{dep})	1073 K
Total pressure (P_{tot})	0.8 kPa
Temperature of nozzle (T_{nozzle})	693 K
Deposition time (t_{dep})	0.9 ks
Flow rate of carrier gas	
Ar gas for Zr precursor (FR_{Zr})	8.33×10^{-7} m^{3}s^{-1}
Ar gas for Y precursor (FR_Y)	8.33×10^{-7} m^{3}s^{-1}
Flow rate of oxygen (FR_{O_2})	8.33×10^{-7} m^{3}s^{-1}
Total gas flow rate (FR_{tot})	3.33×10^{-6} m^{3}s^{-1}

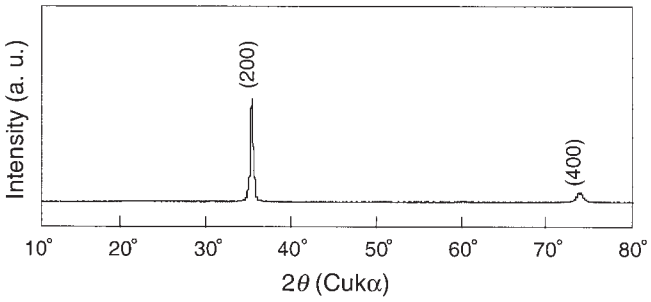

Fig. 12 X-ray diffraction pattern of YSZ film containing 8 mol% Y_2O_3.

diffraction pattern of the YSZ film. All peaks were identified as cubic zirconia, and significant (100) orientation was observed.

Figure 13 represents the surface and cross section of YSZ film after corrosion at 1273 K and $P_{SO_2} = 10$ kPa for 43 ks. No cracks, no pores and no structural changes were observed after the corrosion experiments. A dense oxide layer (mainly Cr_2O_3) was observed between the YSZ film and the substrate. As mentioned above, the alloy specimens were pre-oxidized before coating to obtain a well-adhered coating. Comparison of Fig. 11(b) and Fig. 13(b) shows that the dense interface oxide layer became thicker as a result of the corrosion experiments. YSZ films are widely used as thermal barrier coatings for Ni-based alloys.[14,15] It is well known that oxide layers grow at the YSZ/alloy interface due to the diffusion of oxygen through YSZ film. In the present study, the dissociated oxygen in Ar–SO_2 atmosphere was able to diffuse to the YSZ/alloy interface, resulting in formation of an oxide layer. No sulfur was detected by EPMA in the YSZ film and alloy substrate as shown in Fig. 13. It is therefore concluded that the YSZ coating has excellent corrosion resistance in an SO_2 atmosphere up to 1273 K.

Yu *et al.* reported that YSZ films were corroded and formed $Zr_3Y_4S_{3.5}O_{9.4}$ at 1173 K in an H_2S–H_2 atmosphere.[16] YSZ may be reactive with H_2S, and the O atoms in YSZ were partially substituted by S atoms in the reduction atmosphere. In the present study where the equilibrium P_{O_2} and P_{S_2} were $10^{-3.58}$ and $10^{-3.88}$ Pa, respectively, no corrosion product

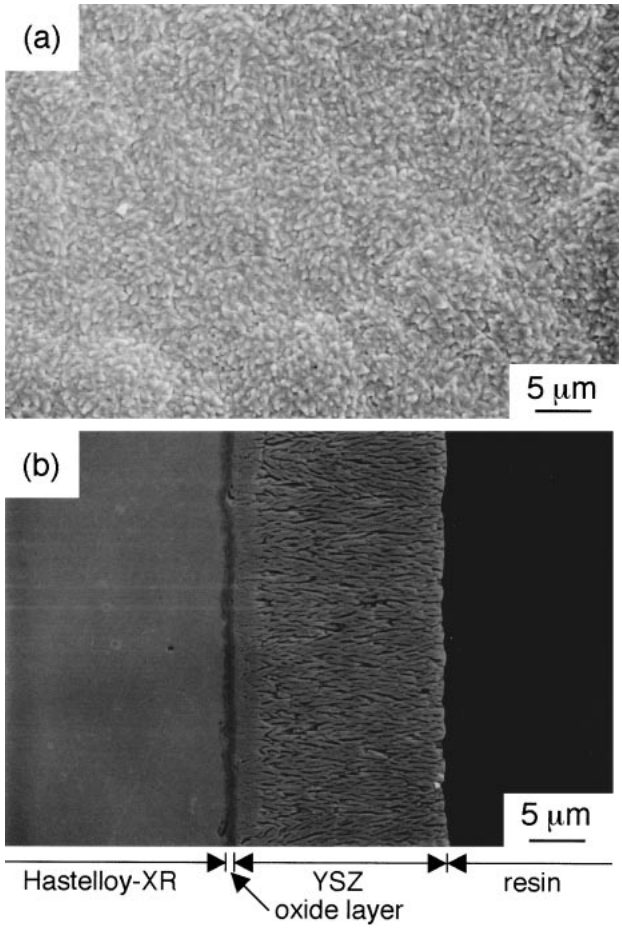

Fig. 13 Surface (a) and cross section (b) of YSZ-coated Hastelloy-XR after corrosion at 1273 K and $P_{SO_2} = 10$ kPa for 43 ks.

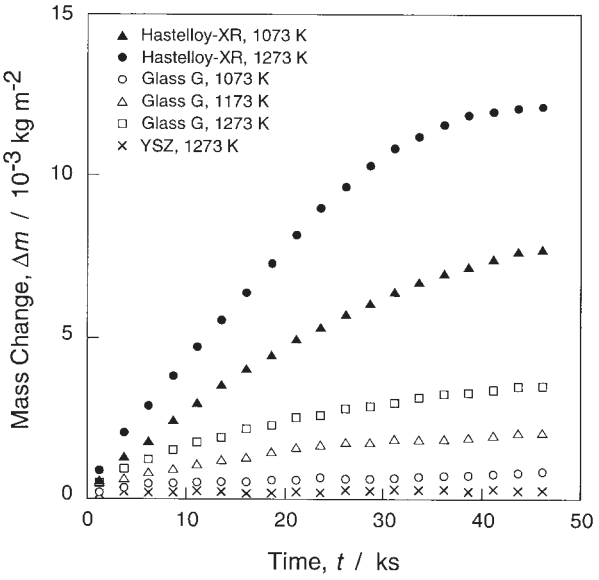

Fig. 14 Mass gain of glass G and YSZ coated Hastelloy-XR after corrosion at 1073 to 1273 K and $P_{SO_2} = 10$ kPa for 43 ks.

such as $Zr_3Y_4S_{3.5}O_{9.4}$ resulting from the slight oxidative atmosphere was observed.

Figure 14 shows the relationship between mass gain and time for glass-lined, YSZ-coated alloys during corrosion at 1073 to 1273 K and at $P_{SO_2} = 10$ kPa for 43 ks. The mass gain of glass G lining alloys was significantly smaller than that of bare Hastelloy-XR alloy. The glass G lining significantly improved the corrosion resistance below 1073 K. The YSZ coating was more effective than the glass lining in an SO_2 atmosphere showing almost no mass change at 1273 K.

4. Conclusions

Glass linings and YSZ coatings were applied to improve the corrosion resistance of Hastelloy-XR alloy in an SO_2 atmosphere. A glass with a composition of 48 SiO_2–8 B_2O_3–6 Al_2O_3–11 CaO–25 BaO–2 ZnO (mass%) adhered well to the alloy substrate and showed almost no degradation and no mass change below 1073 K. The YSZ (8 mol% Y_2O_3) coating prepared by CVD had a well-grown columnar structure and showed excellent corrosion resistance at 1273 K.

Acknowledgments

This work was performed as a part of Nanostructure Coating Project carried out by the New Energy and Industrial Technology Development Organization (NEDO), Japan. The authors wish to thank Mr. Y. Murakami of the Laboratory for Advanced Materials, Institute for Materials Research, for EPMA analyses. One of the authors (R. Tu) is grateful to the Tokyu Foundation for Inbound Students.

REFERENCES

1) J. Funk and M. Reinstrom: I&EC Process Design and Develop. **5** (1966) 336–342.
2) A. Hammache and E. Bilgen: J. Energ. Resources Tech. **114** (1992) 227–234.
3) C. Berndhauser and K. F. Knoche: Int. J. Hydrogen Energy **19** (1994) 239–244.
4) Y. Kurata, K. Tachibana and T. Suzuki: J. Japan Inst. Metals **65**(4) (2001) 262–265.
5) T. Goto: Materia Japan **40** (2001) 368–371.
6) Y. Imai, S. Mizuta and H. Nakauchi: Boshoku Gijutsu **35** (1986) 230–240.
7) F. Coen Porisini: Int. J. Hydrogen Energy **14** (1989) 267–273.
8) Y. Kurata and H. Nakajima: J. Nucl. Mater. **228** (1996) 176–183.
9) R. Tu, T. Goto, L. D. Chen, T. Hirai and L. M. Zhang: Mater. Trans. **42** (2001) 2093–2097.
10) R. Tu and T. Goto: J. Mater. Sci. Tech. **19**(1) (2003) 19–22.
11) R. Tu, T. Kimura and T. Goto: Mater. Trans. **43**(9) (2002) 2354–2356.
12) A. A. Appen: *Chemistry of Glass*, (Nisso Tsusinnsya, 1974) pp. 318–323.
13) T. M. Besmann: ORNL/TM-5775, (1977).
14) U. Schulz, M. Menzebach, C. Leyens and Y. Q. Yang: Surface and Coating Tech. **146–147** (2001) 117–123.
15) E. P. Busso, J. Lin, S. Sakurai and M. Nakayama: Acta Mater. **49** (2001) 1515–1528.
16) Z. Yu, H. Taumi and T. Narita: Zairyo-to-Kankyo **50** (2001) 376–379.